

Effect of contact time, temperature and pH of dyes to be adsorbed on the mesoporous silica used for water treatment

Mayank*

*Associate Professor Department of Chemistry, Multanilal Modi College, Modinagar, Ghaziabad, UttarPradesh, 201204 India

ABSTRACT

The adsorption behavior of the polyamine functionalized mesoporous silica (MSPEI) is assessed against anionic dyes. The adsorbent characteristics of MS-PEI are compared with a monolayer platform comprising of 3-aminopropyltriethoxy silane (APTES) functionalized mesoporous silica (MS-APTES). A novel branched polyamine (polyethyleneimine, PEI) functionalized mesoporous silica (MS) adsorbent is developed via a facile “grafting-to” approach. X-ray spectroscopy and infrared spectroscopy verified the effective surface fictionalization of MS with monolayer and polymer. The adsorption behavior of the MS-PEI and MS-APTES toward anionic dyes is further evaluated by studying the effect of adsorbent dosage and pH. Langmuir and Freundlich isotherm models are employed to understand the adsorption mechanism. The obtained kinetic data support a pseudo-second order adsorption behavior for both monolayer and polymer functionalized MS.

KEYWORDS: surface modification, adsorbent, water mesoporous silica, branched polyamine, remediation.

INTRODUCTION

Mesoporous silica based materials are being investigated for a variety of different applications such as catalysis (1), drug delivery(2), adsorption (3) and separation(4). These materials are typically synthesized with tunable pore size and geometry in the presence of different cationic/anionic surfactants, which act as templates (5,6). A large variety of mesoporous silica including hexagonal, cubic, dodecagonal, or platelet geometries has been investigated for various applications. The hexagonal MCM-41 mesoporous silica has been prepared by using cationic surfactants as cetyltrimethylammonium bromide (CTAB)(7). Mesoporous materials have emerged as promising adsorbents for the water remediation and offer advantages such as high surface area, surface reactivity, structural stability, and regular channel- type structures (8–10). It is well-known that silica based materials have a negative charge surface due to the presence of Si–OH groups, which prevents the adsorption of negatively charged adsorbents (11,12). Therefore, the effectiveness of mesoporous silica in the adsorption processes is highly dependent on the surface functionalization of the silica network with functional groups that are suitable for adsorption of Specific substances, A variety of surface functionalized mesoporous silica has been explored for adsorption of heavy metal ions and cationic and anionic organic materials.(13). Among the organic pollutant, dye contaminants have caused serious pollution to water resources and the removal of dyes from wastewater has become a major focus of research. Even the presence of a small concentration of dyes is highly visible and considered to be intolerable (14). Many of these dyes are carcinogenic and toxic. In addition, such dyes are resistant to degradation by light, chemical, biological, and other exposures (15). There are various techniques that are used for the remediation of dye wastewater such as oxidation, ozonation. Among these techniques, adsorption is considered to be the most frequent and proficient method for dye removal from wastewater.

EXPERIMENTAL SECTION

Materials and Methods

Cetyltrimethylammonium bromide (CTAB), aqueous ammonia, tetraethyl orthosilicate, toluene, branched polyethyleneimine, sodium dihydrogen phosphate, sodium hydrogen phosphate, ethanol and methanol were purchased from Sigma Aldrich. The synthesis of Mesoporous Silica (MS) was prepared according to the method previously reported (16). Synthesis of Monoamine Modified Silica (MS-APTES). APTES coated mesoporous silica (MS-APTES) was prepared according to the reported procedure (17). Modification of Silica with Glutaraldehyde (MS-GA). Surface modification of MS-APTES with glutaraldehyde was accomplished according to the previously reported method (18). The dye adsorption capacities of MS-APTES and MS-PEI were studied by using various amounts of adsorbents. Functionalized mesoporous silica particles (5–20 mg) were shaken at room temperature with 10 mL aqueous dye solutions of known initial concentration (15 ppm) at optimized contact time and pH (pH = 6, t = 15 min for ARS while pH = 4, t = 2 min for XO). At the end of the adsorption period, the supernatant solutions were filtered and the concentration of each dye in the supernatant solutions before and after the adsorption was determined using a calibration curve obtained by employing a UV spectrophotometer at λ_{\max} of 470 nm for ARS and 436 nm for XO. The amount of dye adsorbed at equilibrium q_e (mg/g) was calculated from the following equation.

$$q_e = \frac{(C_o - C_e)V}{W} \quad (1)$$

Where q_e is the adsorption capacity (mg/g) of the adsorbent at equilibrium, C_o and C_e (mg/g) are the initial and equilibrium concentrations of solute, V is the volume of the aqueous solution in liters, and W is the mass in grams of the adsorbent used (19).

RESULT AND DISCUSSION

A surfactant based template assisted method was used for the fabrication of MS. The surface functionalization of MS with APTES followed by the reaction with glutaraldehyde led to the MS with surface aldehyde groups. The surface aldehyde groups were subsequently used for covalently tethering the branched PEI at the surface of MS via imine linkage.

Effect of Contact Time:

For an ideal adsorbent for water treatment, it needs to show rapid uptake of pollutants and reach the equilibrium in short time. To investigate the effect of contact time on the adsorption of dyes, the functionalized adsorbents (10 mg for ARS and 5 mg for XO) were added to 10 mL of 15 ppm dye solution for time periods ranging from 5 to 30 min for ARS (at pH = 6) and 1 to 5 min for XO (at pH = 4). It was noticed that, for both dyes, uptake increases with the increase in contact time. However, at any given time point, the MS-PEI exhibited higher removal capacity than APTES. MS-PEI exhibited almost complete adsorption of ARS from 15 ppm solution after 30 min, whereas adsorption was 90% in the case of MS-APTES under similar conditions. Adsorption of XO was up to 88% for MS-PEI and 68% for MS-APTES after 5 min (Fig-1).

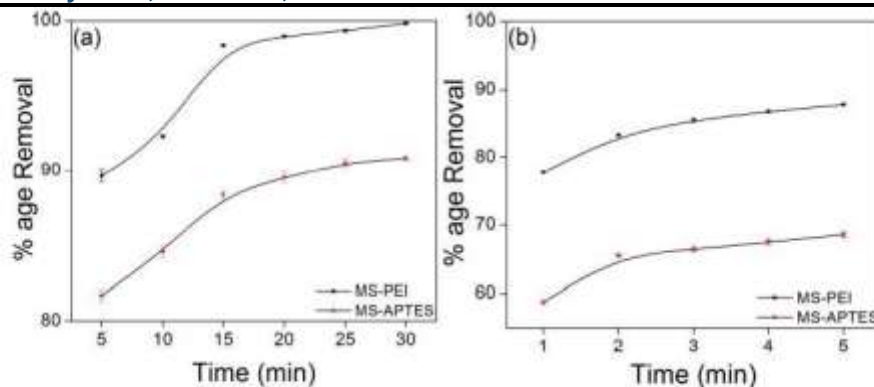


Figure 1. Effect of time on % age of dye removal: ARS (pH = 6, $T = 25\text{ }^{\circ}\text{C}$, amount of adsorbent = 10 mg) (a); XO (pH = 4, $T = 25\text{ }^{\circ}\text{C}$, amount of adsorbent = 5 mg) by MS-APTES and MS-PEI (b). The solid curve is a guide to the eye.

This was the maximum adsorption that could be achieved for both adsorbents in the case of XO, and further increase in contact time did not increase the adsorption indicating the advent of adsorption equilibrium. MS-PEI showed higher adsorption capacity with respect to MS-APTES due to the higher surface functional group density at adsorption sites.

Effect of Temperature:

Temperature has a significant effect on the adsorption process. To study the effect of temperature on the uptake of dyes, adsorption experiments were carried out at different temperatures (ranging from 25 to 65 $^{\circ}\text{C}$). Both adsorbents (10 mg, pH = 6, $t = 15$ min for ARS, and 5 mg, pH = 4, $t = 2$ min for XO) were added to the 10 mL of 15 ppm dye solutions. For both the adsorbents (MS-PEI and MS-APTES), an increase in temperature only slightly decreased the adsorption capacity and maximum adsorption was achieved at room temperature (98% and 88% for ARS and 83% and 65% for XO respectively (Fig- 2).

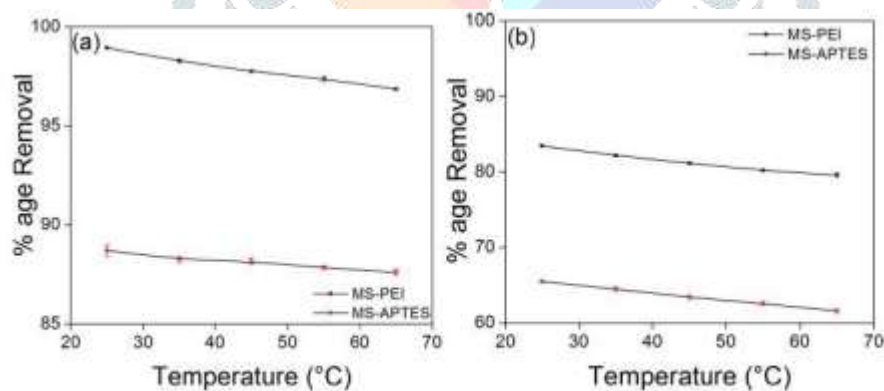


Figure 2. Effect of temperature on % age of dye removal: ARS (pH = 6, $t = 15$ min, amount of adsorbent = 10 mg) (a); XO (pH = 4, $t = 2$ min, amount of adsorbent = 5 mg) by MS-APTES and MS-PEI (b). The solid curve is a guide to the eye.

This behavior revealed an exothermic nature of the adsorption process. The weakening of physical interactions between dyes and active adsorbent sites could be the significant contributor toward a decrease in adsorption capacity with an increase in the temperature. The aqueous solubility of solutes generally increases with the increase in temperature, therefore impeding the adsorption process.

Effect of pH:

The pH of the solution is a key parameter in regulating the adsorption of charged moieties, by altering the surface charge of the adsorbent and the degree of ionization of the dyes. The effect of pH on the adsorption of anionic dyes ARS and XO was studied systematically. For this purpose, solutions were prepared in the pH range of 2–12. The pH of solutions was adjusted by using 0.1 M HCl and 0.1 M NaOH. The adsorption capacity of MS-PEI and MS-APTES toward ARS (15 ppm, 10 mL, $t = 15$ min, 10 mg adsorbent) initially

increased as the pH of the solution was increased from 2 and reached a maximum at 6. At pH 6, the surface positive charge on the adsorbents, due to the protonation of the amino groups, and the negative charge on the ARS seem to be in the right combination to give maximum adsorption (98% for MS-PEI and 88% for MS-APTES). A further increase in the pH resulted in the decrease of adsorption capacity, presumably because of the deprotonation of the surface amino groups and protonation of the acidic functional groups of ARS, leading to an electrostatic repulsion between adsorbent and the adsorbate. A similar trend was observed for the XO (15 ppm, 10 mL, $t = 2$ min, 5 mg adsorbent) where both adsorbents (MS-PEI and MS-PEI) showed maximum adsorption capacity (83% and 65% respectively) at pH 4 (Fig-3).

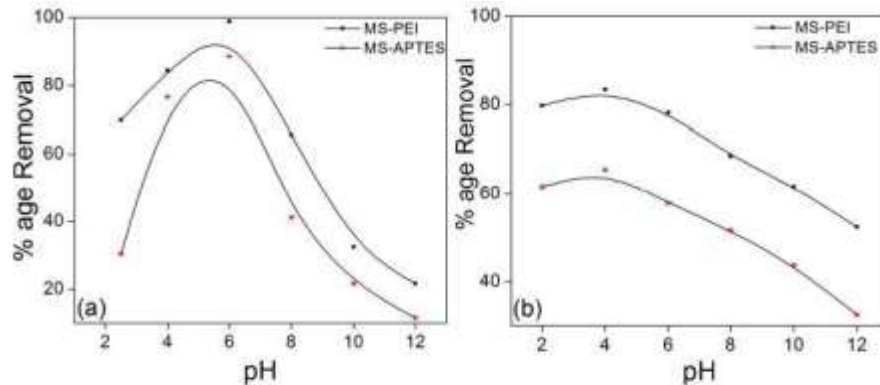


Figure 3. Effect of pH on % dye removal: ARS ($t = 15$ min, $T = 25$ °C, amount of adsorbent = 10 mg) (a); XO ($t = 2$ min, $T = 25$ °C, amount of adsorbent = 5 mg) by MS-APTES and MS-PEI (b). The solid curve is a guide to the eye.

Adsorption Thermodynamics

In order to study the effect of temperature on the adsorption process, the values of the thermodynamic parameters such as the Gibbs' free energy (ΔG°), the standard enthalpy change (ΔH°), and the standard entropy change (ΔS°) were investigated. The magnitude of ΔG° was obtained from the following equation:

$$\Delta G^\circ = - RT \ln K \quad (2)$$

where K is the equilibrium constant, T is the absolute temperature (K), and R is the universal gas constant (8.314 J/mol K).⁴¹ The enthalpy change ΔH° and ΔS° can be obtained from the van't Hoff equation:

$$\ln K = \frac{\Delta S^\circ}{R} - \frac{\Delta H^\circ}{RT} \quad (3)$$

The negative values of ΔG° confirmed that adsorption of dyes on both adsorbents was spontaneous. The negative values of ΔH° indicate the exothermic nature of adsorption processes. The positive values of ΔS° shows the increasing randomness at the surface of adsorbent during adsorption processes, which eventually leads to an increase in the adsorption efficiency. The rate constant (K) for MS-PEI is 2 orders of magnitude higher than the MS-APTES for ARS dye, and it is 1 order of magnitude higher for XO dye. Much larger values of K mean anionic dye adsorption on polyamine functionalized mesoporous nano particles is stronger and almost complete.

Desorption Studies. Sorbent regeneration is important in the estimation of the competitiveness of the adsorbent system. The studies were carried out by employing different organic solvents and also in acidic, neutral, and alkaline media. The desorption of dyes was carried out by separately washing the ARS ($T = 25$ °C, $t = 15$ min) and XO ($T = 25$ °C, $t = 2$ min) loaded adsorbents with 10 mL each of 1 M HCl, 1 M NaOH, methanol, acetic acid, and a mixture of methanol (0.5 mL) with concentrated acetic acid (9.5 mL)⁽²⁶⁾. The concentrations of dyes in the desorbed solutions were determined

spectrophotometrically. The best desorption was achieved with NaOH for both adsorbents. The desorption efficiency was up to 90% for ARS and 55% for XO in the case of MS-PEI adsorbent, while it was 40% for ARS and 20% for XO in the case of MS-APTES. An effect of pH on desorption of dyes in water was also investigated. The primary advantage of adsorption over other processes is subjected to the recycling ability of the adsorbent. The reusability of adsorbent during the adsorption process reduces the operational cost. Therefore, the reusability of MS-PEI and MS-APTES for adsorption of dyes was studied. Desorption of the dyes from the loaded adsorbents was carried out by washing the particles with ethanol before each reusability cycle(27). The results depict superior stability of MS-PEI during the adsorption–desorption cycle and show higher recycling capacity for ARS (7 cycles) and XO (5 cycles), as compared to MS-APTES, which was effective for up to 6 and 3 cycles for ARS and XO, respectively. Thus, MS-PEI is not merely efficient in adsorption but also possesses better potential for reusability.

CONCLUSIONS

A branched polymer PEI was covalently tethered at the surface of mesoporous silica to develop a novel adsorbent system, MSPEI, for water remediation. The effectiveness of the employed strategy for the fabrication of mesoporous adsorbent material was supported by the ATR-FTIR, XPS, and TEM analyses. The adsorption studies of anionic dyes (ARS and XO) on MS-PEI and its monolayer analogue MS-APTES modified silica revealed the superior adsorption characteristics for MS-PEI, which can be attributed to the higher amine group density on the surface of adsorbent. The higher adsorption capacity toward both the dye molecules may be explained by the electrostatic nature of the interaction between the surface of the adsorbent and anionic dyes. The adsorption capacity was found to increase with the increase in adsorbent dosage and contact time. The solution pH has significant influence on the adsorption processes as an increase in the pH of the solutions led to a significant decrease in adsorption. Maximum adsorption against both adsorbents was achieved at room temperature that slightly decreased with an increase in temperature, reflecting on the exothermic adsorption behaviors. The pseudo-second-order equation gave the better correlation for the adsorption data. The presented results highlight the relevance of the developed branched polymer functionalized mesoporous adsorbent material for environmental remediation by demonstrating the high removal efficiency, controlled adsorption–desorption characteristics, and most importantly reusability performances.

REFERENCES

- (1). Melero, J. A.; van Grieken, R.; Morales, G. Advances in the synthesis and catalytic applications of organosulfonic-functionalized mesostructured materials. *Chem. Rev.* 2006, 106 (9), 3790–3812.
- (2). Tang, F.; Li, L.; Chen, D. Mesoporous silica nanoparticles: Synthesis, biocompatibility and drug delivery. *Adv. Mater.* 2012, 24 (12), 1504–1534.
- (3). Sepehrian, H.; Fasihi, J.; Khayat-zadeh Mahani, M. Adsorption behavior studies of picric acid on mesoporous MCM-41. *Ind. Eng. Chem. Res.* 2009, 48 (14), 6772–6775.
- (4). Ju, Y.; Webb, O.; Dai, S.; Lin, J.; Barnes, C. Synthesis and characterization of ordered mesoporous anion-exchange inorganic/organic hybrid resins for radionuclide separation. *Ind. Eng. Chem. Res.* 2000, 39 (2), 550–553.
- (5). Suteewong, T.; Sai, H.; Hovden, R.; Muller, D.; Bradbury, M. S.; Gruner, S. M.; Wiesner, U. Multicompartment mesoporous silica nanoparticles with branched shapes: An epitaxial growth mechanism. *Science* 2013, 340 (6130), 337–341.
- (6). Che, S.; Garcia-Bennett, A. E.; Yokoi, T.; Sakamoto, K.; Kunieda, H.; Terasaki, O.; Tatsumi, T. A novel anionic surfactant templating route for synthesizing mesoporous silica with unique structure. *Nat. Mater.* 2003, 2 (12), 801–805.
- (7). Tolbert, S. H.; Firouzi, A.; Stucky, G. D.; Chmelka, B. F. Magnetic field alignment of ordered silicate-surfactant composites and mesoporous silica. *Science* 1997, 278 (5336), 264–268.
- (8). He, H.-B.; Li, B.; Dong, J.-P.; Lei, Y.-Y.; Wang, T.-L.; Yu, Q.-W.; Feng, Y.-Q.; Sun, Y.-B. Mesostructured nanomagnetic polyhedral oligomeric silsesquioxanes (POSS) incorporated with dithiol organic anchors for multiple pollutants capturing in wastewater. *ACS Appl. Mater. Interfaces* 2013, 5 (16), 8058–8066.

- (9) Billinge, S. J.; McKimmy, E. J.; Shatnawi, M.; Kim, H.; Petkov, V.; Wermeille, D.; Pinnavaia, T. J. Mercury binding sites in thiolfunctionalized mesostructured silica. *J. Am. Chem. Soc.* 2005, 127 (23), 8492–8498.
- (10) Aguado, J.; Arsuaga, J. M.; Arencibia, A.; Lindo, M.; Gascón, V. Aqueous heavy metals removal by adsorption on amine-functionalized mesoporous silica. *J. Hazard. Mater.* 2009, 163 (1), 213–221.
- (11) Anbia, M.; Salehi, S. Removal of acid dyes from aqueous media by adsorption onto amino-functionalized nanoporous silica SBA-3. *Dyes Pigm.* 2012, 94 (1), 1–9.
- (12) Walcarius, A.; Mercier, L. Mesoporous organosilica adsorbents: Nanoengineered materials for removal of organic and inorganic pollutants. *J. Mater. Chem.* 2010, 20 (22), 4478–4511.
- (13) Lam, K. F.; Yeung, K. L.; McKay, G. Selective mesoporous adsorbents for and Cu²⁺ separation. *Microporous Mesoporous Mater.* 2007, 100 (1), 191–201.
- (14) Zhuang, X.; Wan, Y.; Feng, C.; Shen, Y.; Zhao, D. Highly efficient adsorption of bulky dye molecules in wastewater on ordered mesoporous carbons. *Chem. Mater.* 2009, 21 (4), 706–716.
- (15) Donia, A. M.; Atia, A. A.; Al-amrani, W. A.; El-Nahas, A. M. Effect of structural properties of acid dyes on their adsorption behaviour from aqueous solutions by amine modified silica. *J. Hazard. Mater.* 2009, 161 (2), 1544–1550.
- (16) Lam, K. F.; Yeung, K. L.; McKay, G. Efficient approach for Cd²⁺ and Ni²⁺ removal and recovery using mesoporous adsorbent with tunable selectivity. *Environ. Sci. Technol.* 2007, 41 (9), 3329–3334.
- (17) Lam, K. F.; Yeung, K. L.; McKay, G. An investigation of gold adsorption from a binary mixture with selective mesoporous silica adsorbents. *J. Phys. Chem. B* 2006, 110 (5), 2187–2194.
- (18) Bi, X.; Lau, R. J.; Yang, K.-L. Preparation of ion-imprinted silica gels functionalized with glycine, diglycine, and triglycine and their adsorption properties for copper ions. *Langmuir* 2007, 23 (15), 8079–8086.
- (19) Zhou, L.; Gao, C.; Xu, W. Magnetic dendritic materials for highly efficient adsorption of dyes and drugs. *ACS Appl. Mater. Interfaces* 2010, 2 (5), 1483–1491.

